

# Conformational Effects on the Ultraviolet Absorption Spectrum of *n*-Tetrasilane: Multistate Complete Active Space Second-Order Perturbation Theory Treatment<sup>†</sup>

Mari Carmen Piqueras, Manuela Merchán, and Raúl Crespo\*

Departament de Química Física i Institut de Ciència Molecular, Universitat de València, Dr. Moliner 50, E-46100 Burjassot (Valencia), Spain

Josef Michl\*

Department of Chemistry and Biochemistry, University of Colorado, Boulder, Colorado 80309-0215

Received: February 19, 2002; In Final Form: May 9, 2002

A theoretical analysis and interpretation of the reported UV absorption spectra of the anti and gauche conformers of *n*-tetrasilane is offered, based on the results of multistate complete active space second-order perturbation theory (MS-CASPT2) calculations for their low-energy valence electronic excited states. A generally contracted basis set of atomic natural orbitals (ANOs) and a ground-state geometry optimized at the second-order Möller–Plesset perturbation theory (MP2) level by use of Dunning's correlation-consistent triple- $\zeta$  basis set (cc-pVTZ) have been used. Six valence excited states are calculated for the anti conformer. In terms of natural orbitals they correspond to single-electron promotions from the  $\sigma_1$  highest occupied molecular orbital (HOMO) to four  $\sigma^*$  and two  $\pi^*$  valence orbitals. Eight valence excited states are computed for the gauche conformer. Six of these correlate with the states calculated for the anti conformer, while two are new and correspond to single-electron promotions from the  $\sigma_2$  HOMO-1 to the  $\sigma_1^*$  and  $\sigma_2^*$  valence orbitals. The interpretation of the UV absorption spectrum of *n*-tetrasilane in terms of the present calculations shows strong contributions from six valence states instead of four. The main contribution to the second band is from the gauche conformer and involves an excitation from the  $\sigma_2$  HOMO-1 orbital, which was previously not emphasized. The description of the conformational effects on the spectrum confirms the proposal that the energy of the electronic transitions has a weak dependence on the backbone dihedral angle, while the computed intensity is strongly affected by the conformation.

## Introduction

Spectroscopic properties of polysilanes have been of considerable interest because of their striking electronic absorption in the near UV region.<sup>1</sup> A good understanding of the electronic spectra of the oligomers might help to understand the spectra of the polymers and, in particular, the profound effect that the conformation of the silicon backbone has on their optical properties.<sup>2</sup> It is believed that conformational changes are responsible for the remarkable thermochromism,<sup>3</sup> solvatochromism,<sup>4</sup> and piezochromism<sup>5</sup> of these materials. These effects are quite noteworthy considering that the interconversion of conformers merely involves rotations around single bonds in a saturated structure.

Many theoretical and experimental studies have been carried out in an effort to understand the relation between the spectral properties and conformation of short oligosilane chains, but it has not been resolved fully even for the shortest conformationally dependent system, *n*-tetrasilane (*n*-Si<sub>4</sub>H<sub>10</sub>). Its UV absorption spectrum in cyclohexane contains a broad band with an absorption maximum at 48 700 cm<sup>-1</sup>.<sup>6</sup> This band was at first assigned to Rydberg excitation by some authors<sup>7,8</sup> and to valence excitation by others.<sup>9,10</sup> In a nitrogen matrix, broad bands are observed at 49 500 and 55 600 cm<sup>-1</sup>, and photolysis followed by UV and IR spectroscopy demonstrated directly that a mixture

of gauche and anti conformers is present.<sup>11</sup> The former was not found to absorb at substantially higher energies than the latter, contrary to expectations that were common at the time<sup>1</sup> and in partial agreement with early calculations,<sup>9,10</sup> which suggested that the difference would be only 0.3–0.5 eV. The nearly complete overlap of the absorptions of the two conformers agreed with the proposal<sup>12</sup> that it would be the intensity of the low-energy excited singlet states, rather than their energy, that should be a sensitive function of the SiSiSiSi dihedral angle. This reinterpretation was based on the results of CIS calculations that predicted an avoided crossing between a  $\sigma\sigma^*$  B state and a  $\sigma\pi^*$  B state as the dihedral angle goes from the syn to the anti extreme. They also predicted the presence and a similar avoided crossing of two states of A symmetry in the same spectral region.<sup>12</sup> Because of their very weak calculated intensity, these would presumably be hard to observe. Similar results were obtained later at the CASSCF level of theory.<sup>11</sup> Additional support for this proposal was found in the UV spectra of the conformers of matrix-isolated permethyl-*n*-tetrasilane, *n*-Si<sub>4</sub>Me<sub>10</sub>,<sup>13</sup> and more recently from a comparison of the absorption spectra of a series of peralkylated tetrasilanes with constrained silicon backbone dihedral angles,<sup>14,15</sup> which also permitted a direct observation of the lower of the two predicted weak transitions into states of A symmetry.

The early theoretical studies accounted only qualitatively for the observed conformational dependence of condensed-phase UV absorption spectra, as the computed excitation energies were

<sup>†</sup> Part of the special issue "Jack Beauchamp Festschrift".

\* Corresponding authors: e-mail michl@eefus.colorado.edu or Raul.Crespo@uv.es.

too high. Also, they did not entirely clarify the possible intervention of Rydberg states in the observed condensed-phase spectra. Indeed, in at least one of them,<sup>10</sup> the computed lowest Rydberg states of *n*-tetrasilane were of comparable energy as the lowest valence states. A CIS study using a large basis set including Rydberg orbitals<sup>16</sup> showed that the first two excited states are of valence nature at all dihedral angles in the isolated molecule, and that the lowest four states are of valence character when the molecule is embedded in a rare gas cluster. The results showed that a basis set without Rydberg functions was adequate for the computation of the low-energy parts of the condensed-phase spectra.

A recent MS-CASPT2 study of the anti conformer of *n*-tetrasilane<sup>17</sup> suggested that the current description<sup>11–14,16</sup> of its singlet–singlet valence electronic transitions requires yet another level of refinement: six, instead of four, valence excited states are located below the lowest Rydberg state. In the present study, we are following up on this hint by extending our investigations to the gauche conformer. Because of the absence of substituents, the parent *n*-tetrasilane, *n*-Si<sub>4</sub>H<sub>10</sub>, is the ideal system for reaching conclusive interpretations of the conformational effects and also is the one for which the highest level calculations are possible. Unfortunately, experimental work with it is difficult. We interpret and assign the two observed absorption bands and discuss the nature of the low-lying valence excited states and the previously proposed assignments.

The present study also provides an additional test of the general validity of the computational methodology that we found necessary to obtain accurate results in our previous work on the UV absorption spectra of trisilane<sup>18</sup> and the anti conformer of *n*-tetrasilane.<sup>17</sup> In these papers, it was determined that the ordinary multiconfigurational second-order perturbation theory (CASPT2) was insufficient because of the coupling between the different excited states. It was found that in order to obtain accurate results the multistate complete active space second-order perturbation (MS-CASPT2) method needs to be employed. This treats all states of a particular symmetry class simultaneously, with the correlation effects on the reference function included. The method and computational details are described in the next section.

### Computational Methods

The equilibrium geometries of the ground state of the gauche and anti conformers of *n*-tetrasilane were determined by the second-order Möller–Plesset perturbation theory with frozen core, MP2(fc), using Dunning's correlation-consistent triple- $\zeta$  basis set (cc-pVTZ),<sup>19</sup> 5s2p2d1f for the silicon atoms and 3s2p1d for the hydrogen atoms. This choice was based on a recent study of the electronic absorption spectrum of trisilane,<sup>18</sup> which demonstrated its suitability and reliability for obtaining accurate geometrical parameters for oligosilanes. The geometry of the gauche conformer was optimized within the constraint of *C*<sub>2</sub> symmetry point group, with the *z* axis along the *C*<sub>2</sub> symmetry axis direction. That of the anti conformer was optimized in the *C*<sub>2h</sub> group, with the silicon atoms in the *xy* plane and the *y* axis parallel to the terminal Si–Si bonds. MP2 vibrational frequencies were calculated at both optimized structures to confirm that they were minima on the potential energy surface. All these calculations used the Gaussian 98 suite of programs.<sup>20</sup>

At the optimized geometries, electronic properties were computed from complete active space self-consistent field (CASSCF) wave functions employing a generally contracted basis set of atomic natural orbitals (ANOs) obtained from Si(17s12p5d4f)/H(8s4p) primitive sets<sup>21</sup> by use of the Si[6s5p2d1f]/H[3s1p] contraction scheme. The basis set did not

include Rydberg functions because of the results obtained in a previous investigation of the anti conformer of *n*-tetrasilane,<sup>16,17</sup> which showed that even the largest differences between the energies and oscillator strengths of the valence excited states calculated with or without Rydberg functions in the basis set were well within the accuracy of the method. A good description of the valence excited states can therefore be achieved at a lower computational cost.

The calculations for both conformers were performed within the *C*<sub>2</sub> symmetry point group to facilitate comparison. The reference wave function and the molecular orbitals were obtained from average CASSCF calculations, in which the averaging included all the A and B symmetry states of interest. All four 1s core orbitals of the silicon atoms were kept frozen in the form determined by the ground-state SCF wave function. The active space used in all calculations was (5,4), where we specify the numbers of active orbitals belonging to the irreducible representations of the *C*<sub>2</sub> point group a and b, respectively. These were chosen so as to include the  $\sigma$  and  $\sigma^*$  Si–Si bond orbitals and the  $\pi^*$  Si–H bond orbitals, based on our previous experience with CASPT2 calculation of the electronic spectrum of the anti conformer of *n*-tetrasilane.<sup>17</sup> In all calculations the number of active electrons was set to six, which corresponds to the three Si–Si bonds of the  $\sigma$ -conjugated system of the molecule.

To account for the remaining dynamical correlation effects, single-state second-order perturbation theory with a multi-configurational reference state, the CASPT2 approach,<sup>22</sup> was used. This method calculates the first-order wave function and the second-order energy with a CASSCF<sup>23</sup> wave function as the reference. The coupling of the CASSCF wave functions by dynamic correlation was evaluated by the extended multistate CASPT2 (MS-CASPT2) method.<sup>24</sup> In the MS-CASPT2 approach an effective Hamiltonian is computed perturbatively and diagonalized within a multidimensional reference space, permitting the state-average CASSCF states to interact. This allows a simultaneous treatment of all states of a particular symmetry class, including the correlation effects on the reference functions. As a consequence, the MS-CASPT2 method provides an accurate description of the electronic states in cases where several states of the same symmetry need to be treated simultaneously, as is the case in spectroscopic applications. The MS-CASPT2 method gave good results for the anti conformer of *n*-tetrasilane<sup>17</sup> and trisilane,<sup>18</sup> where average CASSCF calculations introduced artifactual valence–Rydberg mixing. We expect to find a similar situation in this study and think that the MS-CASPT2 method will be able to remove the possible erratic mixing due to the presence of somewhat diffuse polarization functions. Additional intruder states weakly interacting with the reference CASSCF wave function were handled by the level shift technique.<sup>25</sup> A level shift of 0.05 au has been used in all calculations in order to remove all intruder-state problems, without affecting the excitation energies by more than 0.1 eV.

The CASSCF state interaction (CASSI) method was employed to compute the transition dipole moments, which were combined with MS-CASPT2 energy differences to obtain the oscillator strengths. The MS-CASPT2 oscillator strength were obtained by use of the perturbation-modified CAS (PMCAS) reference functions<sup>24</sup> obtained as linear combinations of all CAS states involved in the MS-CASPT2 calculation. This procedure has been well established in the study of electronic excitation spectra of oligosilanes.<sup>17,18</sup> The MS-CASPT2 calculations were performed with the MOLCAS-5 quantum chemistry software.<sup>26</sup>

**TABLE 1: MP2(fc)/cc-pVTZ Optimized Ground-State Geometry for the Anti ( $C_{2h}$ ) and Gauche ( $C_2$ ) Conformers of  $n$ -Tetrasilane**

parameter <sup>d</sup>	anti	gauche	exp <sup>b</sup>
$r_{\text{Si}(1)\text{Si}(2)}$	2.350	2.351	2.335(3)
$r_{\text{Si}(2)\text{Si}(3)}$	2.350	2.350	2.340(3)
$r_{\text{Si}(1)\text{Si}(3)}$	3.868	3.843	3.820(5)
$r_{\text{Si}(1)\text{Si}(4)}$	5.953	4.472	5.884(7) <sup>c</sup> ; 4.248(8) <sup>d</sup>
$r_{\text{Si}(1)\text{H}(1)}$	1.481	1.481	1.473(3)
$r_{\text{Si}(2)\text{H}(2)}$	1.484	1.484	1.477(2)
$\angle\text{Si}(1)\text{Si}(2)\text{Si}(3)$	110.8	109.7	109.6(2)
$\angle\text{Si}(2)\text{Si}(1)\text{H}(1)$	110.8	109.7	111.9(9)
$\angle\text{Si}(1)\text{Si}(2)\text{Si}(3)\text{Si}(4)$	180	57.5	180 <sup>c</sup> ; 44(13) <sup>d</sup>

<sup>a</sup> Distances are given in angstroms, and angles are given in degrees.

<sup>b</sup> From ref 27. <sup>c</sup> Anti conformer. <sup>d</sup> Gauche conformer.

## Results

For both the anti and gauche conformers of  $n$ -tetrasilane, Table 1 shows an agreement between the optimized geometrical parameters calculated for the ground-state structure and those deduced from gas electron diffraction,<sup>27</sup> within 0.015 Å for bond lengths and within 2.5° for bond angles. The results for the anti conformer compare very well with our previously computed values<sup>16</sup> but are in even better agreement with the experimental data. The results for both conformers also agree well with those of other earlier calculations.<sup>28,29</sup> The value of 57.5° calculated for the SiSiSiSi dihedral angle for the gauche conformer lies within the experimental error of the observed value, 44° ± 13°.<sup>27</sup> Even the experimental and calculated values for the long nonbonded distance between the two terminal silicon atoms agree well for both the anti (5.885 and 5.953 Å, respectively) and gauche (4.249 and 4.472 Å, respectively) conformers. The good agreement between calculated and experimental data indicates that the computational level allows an accurate description of these molecules and reinforces our previous conclusions<sup>18</sup> concerning the reliability of the geometrical parameters obtained at the MP2/cc-pVTZ level for oligosilanes.

Table 2 collects the vertical excitation energies of the singlet valence states of the gauche and anti conformers of  $n$ -tetrasilane calculated at the MS-CASPT2 level, together with their respective oscillator strengths and the results of our previous calculations on the anti conformer.<sup>17</sup> In our previous study of the anti conformer of  $n$ -tetrasilane we found six valence excited states below the lowest Rydberg transition, located at 7.40 eV. The first ionization potentials of the anti and gauche conformers calculated at the CASPT2 level are 9.37 and 9.57 eV, respectively. Then, we conclude that the lowest Rydberg transition of the gauche conformer must be located above 7.40 eV. Since the reported UV absorption spectrum of  $n$ -tetrasilane shows two main bands with maxima at 49 500 cm<sup>-1</sup> (6.14 eV) and 55 600 cm<sup>-1</sup> (6.89 eV), Table 2 includes the energies of the lowest six valence states computed for the anti conformer and the lowest eight valence states of the gauche conformer, which must be primarily responsible for the two observed bands. We have recomputed the energies and oscillator strengths of the anti conformer at the improved geometry and with the present larger basis set in order to provide a consistent comparison with the energies calculated for the gauche conformer.

**The Anti Conformer.** The properties of the anti conformer computed previously<sup>17</sup> by use of the MP2(fc)/MC-311G\* optimized geometry and the Si[6s5p2d]/H[2s1p] ANO-type basis set and those calculated now with the MP2(fc)/cc-pVTZ optimized geometry and the Si[6s5p2d1f]/H[3s1p] ANO-type basis set are quite similar (Table 2), demonstrating the stability

of the procedure used. The main difference is that the present calculations locate the states about 0.2 eV lower in energy, except for the excitation energies of the two A<sub>g</sub> states, which are almost identical in both approaches. The maximum difference between the energies of the excited states in the two calculations is observed for the 2<sup>1</sup>B<sub>u</sub> state (0.24 eV). The oscillator strengths and transition moment directions of transitions that have significant intensity are nearly the same in both calculations. The transition into the 1<sup>1</sup>B<sub>u</sub> state is polarized approximately along the Si(1)Si(4) line, and that into the 2<sup>1</sup>B<sub>u</sub> state, approximately along the Si(2)Si(3) line. The reduction of the lowest excitation energy from the previously calculated value of 6.36 eV<sup>17</sup> to the present value of 6.15 eV brings it into better agreement with the experimental value of 6.14 eV. Clearly, the use of the MP2/cc-pVTZ geometry in conjunction with the Si[6s5p2d1f]/H[3s1p] ANO-type basis set is superior, confirming the observations made previously in the study of trisilane.<sup>18</sup>

As noted in our previous paper,<sup>17</sup> the description provided by the MS-CASPT2 method for electronic excitations in *anti*- $n$ -tetrasilane differs in two ways from that obtained previously at lower levels of theory. First, calculations by the CIS<sup>12,16</sup> and CASSCF<sup>11</sup> methods provided an only qualitatively correct description of the observed spectra and yielded excitation energies that were too high. Second, they predicted only two A and two B symmetry states of valence nature, whereas the MS-CASPT2 method assigns valence character to the lowest six excited states. Four are the same as before; one of the additional states is of A and the other of B symmetry. The differences are attributable to the lack of dynamic correlation and to the valence–Rydberg mixing that occur at the CASSCF and CIS levels, but they are rectified at the MS-CASPT2 level.

**The Gauche Conformer.** Results for the lowest eight valence excited states are shown in Table 2, to include the six that correlate with the valence states calculated for the anti conformer. Four states are of A and four of B symmetry, and three states of each symmetry correlate with those of the anti conformer. Both additional states are due to excitation from the HOMO-1. The differences between the excitation energies calculated for both conformers are very small, and the first transition in the gauche conformer lies only 0.07 eV above that of the anti conformer. All the states are computed to lie in a narrow energy interval of less than 1 eV, 6.22–7.09 eV for the gauche, and 6.15–6.93 eV for the anti conformer. There are two significant differences with respect to the main features observed for the anti conformer, and they are related to the calculated oscillator strengths and to the NOs of the excited states. In the gauche conformer, all electronic transitions are dipole-allowed, while in the anti form, only three are. In the former, four transitions have large oscillator strength, instead of only two in the latter. All the states of the gauche form are located in two well-defined energy regions, one at 6.2–6.3 eV and the other at 6.7–6.9 eV. The transition moments into the B states tend to cluster around the directions of the Si(2)Si(3) and Si(1)Si(4) lines.

The first electronic transition (into the 1<sup>1</sup>B state) occurs at 6.22 eV and is one of the two most strongly allowed, with an oscillator strength of about 0.4. Even so, its intensity is less than half that calculated for the first electronic transition in the anti conformer (into the 1<sup>1</sup>B<sub>u</sub> state). The second excited state (2<sup>1</sup>A) is very close in energy to the 1<sup>1</sup>B state and carries negligible oscillator strength.

The next electronic transition, from the ground state to the 2<sup>1</sup>B excited state, is the first that belongs to the group located around 6.8 eV. It is calculated to lie at 6.71 eV and has a



**TABLE 2: MS-CASPT2 Vertical Excitation Energies (*E*), Oscillator Strengths (*f*), and Polarization Directions ( $\alpha$ ) of Electronic Transitions in Anti and Gauche Conformers of *n*-Tetrasilane**

gauche				anti				anti <sup>a</sup>		
state	<i>E</i> (eV)	<i>f</i>	$\alpha^b$ (deg)	state	<i>E</i> (eV)	<i>f</i>	$\alpha^b$ (deg)	<i>E</i> (eV)	<i>f</i>	$\alpha^b$ (deg)
1 <sup>1</sup> B ( $\sigma_1 \rightarrow \sigma_1^*$ )	6.22	0.412	19	1 <sup>1</sup> B <sub>u</sub> ( $\sigma_1 \rightarrow \sigma_1^*$ )	6.15	1.027	35	6.36	1.175	37
2 <sup>1</sup> A ( $\sigma_1 \rightarrow \sigma_2^*$ )	6.33	0.040		1 <sup>1</sup> A <sub>u</sub> ( $\sigma_1 \rightarrow \pi_1^*$ )	6.47	0.014		6.66	0.002	
2 <sup>1</sup> B ( $\sigma_1 \rightarrow \pi_2^*$ )	6.71	0.150	-14	2 <sup>1</sup> A <sub>g</sub> ( $\sigma_1 \rightarrow \sigma_2^*$ )	6.62	0		6.68	0	
3 <sup>1</sup> A ( $\sigma_1 \rightarrow \pi_1^*$ )	6.79	0.0001		2 <sup>1</sup> B <sub>u</sub> ( $\sigma_1 \rightarrow \sigma_3^*$ )	6.68	0.141	-35	6.92	0.165	-17
3 <sup>1</sup> B ( $\sigma_2 \rightarrow \sigma_2^*$ )	6.79	0.422	12	3 <sup>1</sup> A <sub>g</sub> ( $\sigma_1 \rightarrow \sigma_4^*$ )	6.87	0		6.96	0	
4 <sup>1</sup> A ( $\sigma_1 \rightarrow \sigma_4^*$ )	6.88	0.154		1 <sup>1</sup> B <sub>g</sub> ( $\sigma_1 \rightarrow \pi_2^*$ )	6.93	0		7.12	0	
5 <sup>1</sup> A ( $\sigma_2 \rightarrow \sigma_1^*$ )	6.91	0.003								
4 <sup>1</sup> B ( $\sigma_1 \rightarrow \sigma_3^*$ )	7.09	0.068	41							

<sup>a</sup> From ref 17. <sup>b</sup> The angle between the transition moment and the direction of the central Si(2)Si(3) bond, both located in the *xy* plane; taken positive if the moment is inclined toward the projection of the Si(1)Si(4) line into the *xy* plane (in the anti conformer, these atoms lie in the *xy* plane). Transition moments into states of A and A<sub>u</sub> symmetries lie in the *z* axis.

significant oscillator strength of 0.15. A transition into the 3<sup>1</sup>A state follows at 6.79 eV, with a very small oscillator strength. The next electronic transition is to a B state (3<sup>1</sup>B) and has a very similar excitation energy (6.79 eV). It is one of the two most strongly allowed, with an oscillator strength of about 0.4. This is the first electronic excitation originating from the HOMO-1. The last member of this group of three states is the 4<sup>1</sup>A, located at 6.88 eV and carrying an oscillator strength of about 0.15. The last two electronic transitions are to the 5<sup>1</sup>A and 4<sup>1</sup>B states, located at 6.91 and 7.09 eV, respectively, and have very small oscillator strength. The transition into the 5<sup>1</sup>A state is the other excitation that originates in the HOMO-1.

## Discussion

**Comparison with Experiment.** To compare the calculated and observed spectra, information is needed about the ratio of the two conformers in the observed sample. Statistically, the gauche conformer is favored by a factor of 2. A gas-phase electron diffraction study of *n*-Si<sub>4</sub>H<sub>10</sub> indicates that at room temperature the gas consists of a 1:2 mixture of the anti and gauche conformers.<sup>27</sup> MP2 calculations<sup>11,29</sup> also suggest a negligible energy difference between them. However, in the nitrogen matrix, the anti conformer is clearly somewhat more stable than the gauche,<sup>11</sup> presumably because the less compact anti form benefits from differential stabilization by intermolecular van der Waals attractions. In the absence of more reliable information, we shall assume that the amounts of the two conformers in the matrix are equal.

Figure 1 compares the UV absorption spectrum of the initially deposited *n*-tetrasilane in N<sub>2</sub> matrix at 12 K, with its two bands at 49 500 cm<sup>-1</sup> (6.14 eV) and at 55 600 cm<sup>-1</sup> (6.89 eV),<sup>11</sup> with a simulation obtained from the MS-CASPT2 calculations, neglecting solvent effects and assuming the spectral line shapes to be Gaussian functions with a full width at half-maximum of 0.3 eV, the same as we used in our treatment of the UV spectrum of trisilane.<sup>18</sup> The contributions of the two conformers are also shown separately. The agreement of the experimental and the computed spectrum is remarkable with respect to both the absolute position and the relative intensities of the two absorption bands (note that a strongly sloping baseline due to light scattering by the matrix has not been subtracted from the measured spectrum). The excellent agreement permits us to propose an interpretation of both observed bands.

The first band is mainly due to two electronic transitions, one from each conformer. The dominant one is the very strongly allowed excitation of the anti conformer to its 1<sup>1</sup>B<sub>u</sub> valence state located at 6.15 eV. The minor one is the about 2.5 times weaker excitation of the gauche conformer to its 1<sup>1</sup>B valence state, computed to lie at 6.22 eV. The other two electronic transitions

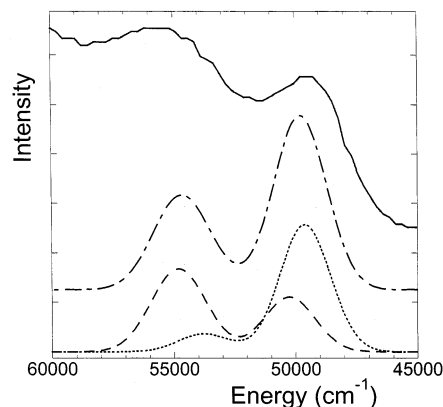


**Figure 1.** MS-CASPT2 simulation of the contributions of the low-energy valence states to the absorption spectrum of *n*-tetrasilane (— · — · —), vacuum ultraviolet absorption spectrum (—),<sup>11</sup> and contributions from the anti (····) and gauche (---) conformers. A full width at half-maximum of 0.3 eV has been assumed.

that occur in this region, into the valence 2<sup>1</sup>A (gauche) and 1<sup>1</sup>A<sub>u</sub> (anti) states, are extremely weakly allowed and make an entirely negligible contribution to the observed band.

The second UV absorption band is due to a superposition of four transitions, one in the anti conformer and three in the gauche. The main contributor to the band is the quite strongly allowed electronic transition into the 3<sup>1</sup>B valence state of the gauche conformer at 6.79 eV. This transition is calculated to originate in excitation of an electron from the HOMO-1 and has not been emphasized before in theoretical studies of the conformational dependence of the electronic states of *n*-tetrasilane.<sup>11,16</sup> The other three contributions to the band are from the 2<sup>1</sup>B<sub>u</sub> state of the anti conformer, located at 6.68 eV, and from the 2<sup>1</sup>B and 4<sup>1</sup>A states of the gauche conformer, computed at 6.71 and 6.88 eV, respectively. These three electronic transitions have very similar oscillator strengths, about 3 times smaller than that carried by the 3<sup>1</sup>B state of the gauche conformer.

To summarize, the lower energy band is primarily due to electronic excitation of the anti conformer, with a significant contribution from the gauche conformer, and the higher energy band is mainly due to excitation of the gauche conformer, with some contribution from the anti conformer. This conclusion is in perfect agreement with the photochemical studies, which showed that irradiation into either band decomposes both conformers. This is true even of irradiation into the red edge of the first observed absorption band at 46 770 cm<sup>-1</sup>, making it clear that the difference in the first excitation energies of the two conformers is very small. However, the destruction occurs to unequal degrees: irradiation at 46 770 or 48 500 cm<sup>-1</sup> (the

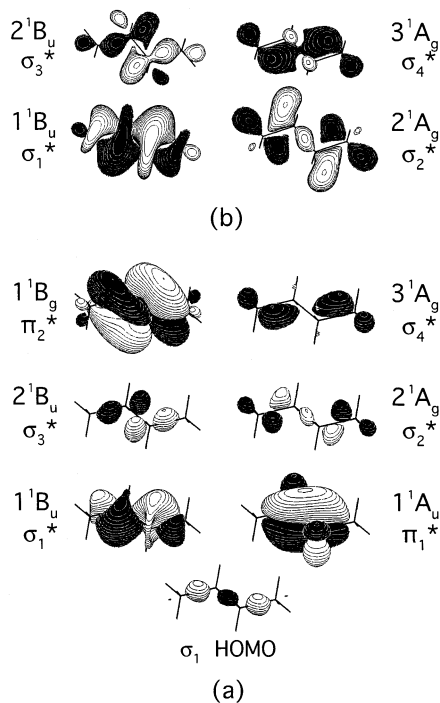


**Figure 2.** Natural orbitals with occupation numbers close to unity obtained from the perturbation-modified CAS (PMCAS) wave functions of the valence-excited states of *anti-n*-tetrasilane. (a) All important NOs (isodensity surface value of 0.02). (b) View of the  $\sigma^*$  NOs along the  $z$  axis (isodensity surface value of 0.015).

first band) destroys mostly the anti conformer, and irradiation at  $54\,080\text{ cm}^{-1}$  (the second band) destroys mostly the gauche conformer.

**Natural Orbital Analysis.** For the anti conformer, the presently obtained natural orbitals of the PMCAS wave functions obtained for the ground and excited states (Figure 2) are very similar to those obtained previously<sup>17</sup> at the MS-CASPT2 level. All the excited states are well represented as one-electron promotions from the highest occupied molecular orbital (HOMO), of  $a_g$  symmetry, into various virtual orbitals. The occupation numbers for both the starting and the terminating NOs of the electronic transitions are close to unity. The NOs look like those anticipated from Hückel theory and do not resemble low-lying virtual SCF orbitals, which contain large diffuse contributions. To display more clearly the nodal properties of the  $\sigma^*$  NOs, they are shown in panel b of Figure 2 in a different perspective and with a different choice of the isodensity surface. The only appreciable difference between the NOs displayed in Figure 2 and the ones shown in our previous study is related to the  $2^1A_g$  and  $3^1A_g$  states. In the previous work, these were contaminated by Rydberg contributions or mixed together due to the inclusion of Rydberg functions in the basis set. Now, they more clearly display the anticipated nodal properties.

The natural orbitals of the PMCAS wave functions obtained for the ground and excited states of the gauche conformer are shown in Figure 3. All the excited states again result from one-electron promotions into different virtual orbitals. Six of these are from the HOMO, of  $a$  symmetry, and two from the HOMO-1, of  $b$  symmetry. The occupation numbers are close to unity for both NOs. The HOMO and HOMO-1 orbitals are visually indistinguishable from the corresponding orbitals obtained from closed-shell Hartree–Fock calculations and have the nodal properties expected from Hückel considerations, as do the virtual orbitals. The  $\sigma^*$  NOs obtained for the  $1^1B$  and  $2^1A$  states, which correspond to the first two excitations from the HOMO, cannot

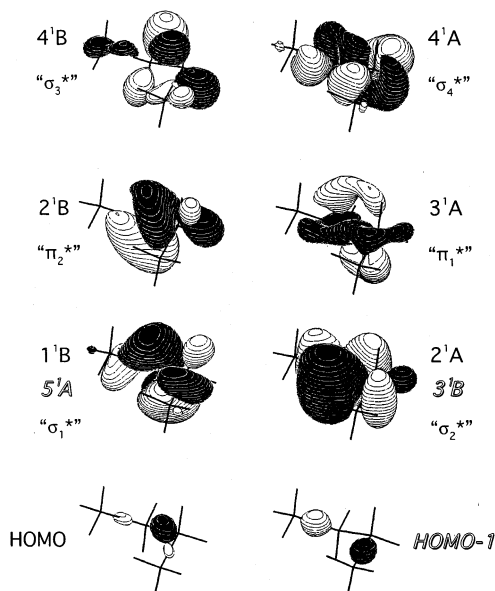


**Figure 3.** Natural orbitals with occupation numbers close to unity obtained from the perturbation-modified CAS (PMCAS) wave functions of the valence-excited states of *gauche-n*-tetrasilane from the HOMO (boldface type) and HOMO-1 (outlined type) to the valence natural orbitals. The isodensity surface value for all the orbitals is 0.02.

be distinguished visually from those obtained for the  $5^1A$  and  $3^1B$  states, respectively, which correspond to the first two electronic transitions from the HOMO-1.

The increased participation of the HOMO-1 in low-energy electronic transitions in the gauche conformer relative to the anti conformer is due to the increase in the energy of this orbital as the SiSiSiSi dihedral angle is reduced. This is well documented both by computations for tetrasilane<sup>29,30</sup> and by experiments on conformationally fixed alkylated tetrasilanes.<sup>31</sup> In simple Hückel terms, it is attributable to vicinal interactions, as formalized in the ladder C model of  $\sigma$  delocalization.<sup>12,32</sup>

Although the symbols  $\sigma$  and  $\pi$  are not strictly applicable to a molecule without a plane of symmetry, they are still applicable qualitatively, and we have marked the NOs shown in Figure 3 accordingly. Note that the polarization direction of the  $\sigma \rightarrow \pi^*$  transition into the  $2^1B$  state is distinctly different from those of the  $\sigma \rightarrow \sigma^*$  transitions into the  $1^1B$  and  $3^1B$  states. The moment of the  $\sigma \rightarrow \sigma^*$  transition into the  $4^1B$  state, which deviates in the opposite direction, is very small and its direction may not be reliable. The similarity between the NOs and the qualitatively anticipated Hückel orbitals is intuitively satisfying but it also suggests that it might be possible to find a simple semiempirical parametrization of the excitation energies in oligosilanes, which might be useful for understanding the intriguing optical properties of polysilanes.

## Conclusions

The results obtained in this study show that the general picture of the electronic excited states of *n*-tetrasilane is more complicated than was previously assumed on the basis of lower level *ab initio* methods. The lowest six and eight excited states of the anti and gauche conformers, respectively, are of valence character, confirming the recent findings for the anti conformer.<sup>17</sup> The current interpretation of the two observed UV absorption bands represents a modification of the previous one,<sup>11–14,16</sup> as now there are six valence excited states from the anti and eight from the gauche conformer that contribute to the observed spectrum, instead of four from each. The most

significant difference in the assignment is the present recognition that the second intense transition of the gauche conformer involves excitation from HOMO-1. Before, this orbital was not considered important for the optical properties of either conformer. The results confirm the current belief that it is the relative transition intensity rather than energy that is remarkably sensitive to the SiSiSiSi dihedral angle.

**Acknowledgment.** This work has been supported by the MCYT Projects BQU2001-2935-CO2-01 and BQU2001-2926 and by the National Science Foundation (CHE-9819179).

## References and Notes

- (1) (a) Miller, R. D.; Michl, J. *Chem. Rev.* **1989**, *89*, 1359. (b) Michl, J.; West, R. In *Silicon-Containing Polymers: the Science and Technology of their Synthesis and Applications*; Jones, R. G., Ando, W., Chojnowski, J., Eds.; Kluwer Academic Publishers: Dordrecht, The Netherlands, 2000; p 499.
- (2) (a) Fujiki, M. *J. Am. Chem. Soc.* **1996**, *118*, 7424. (b) Bukalov, S. S.; Leites, L. A.; West, R.; Aduke, A. *Macromolecules* **1996**, *29*, 907.
- (3) (a) Miller, R. D.; Hofer, D.; Rabolt, J. F.; Fickes, G. N. *J. Am. Chem. Soc.* **1985**, *107*, 2172. (b) Harrah, L. H.; Zeigler, J. M. *J. Polym. Sci., Polym. Lett. Ed.* **1985**, *23*, 209.
- (4) Oka, K.; Fujiue, N.; Dohmaru, T.; Yuan, C. H.; West, R. *J. Am. Chem. Soc.* **1997**, *119*, 4074.
- (5) (a) Schilling, F. C.; Bovey, F. A.; Davis, D. D.; Lovinger, A. J.; MacGregor, R. B., Jr.; Walsh, C. A.; Zeigler, J. M. *Macromolecules* **1989**, *22*, 4645. (b) Song, K.; Kuzmany, H.; Wallraff, G. M.; Miller, R. D.; Rabolt, J. F. *Macromolecules* **1990**, *23*, 3870. (c) Song, K.; Miller, R. D.; Wallraff, G. M.; Rabolt, J. F. *Macromolecules* **1991**, *24*, 4084.
- (6) Freund, R. Ph.D. Dissertation, University of Cologne, Germany, 1973.
- (7) Itoh, U.; Toyoshima, Y.; Onuki, H. *J. Chem. Phys.* **1986**, *85*, 4867.
- (8) Stüger, H.; Hengge, E.; Janoschek, R. *Phosphorus, Sulfur, Silicon* **1990**, *48*, 189.
- (9) Crespo, R.; Piqueras, M. C.; Orti, E.; Bredas, J. L. *Synth. Met.* **1991**, *43*, 3457.
- (10) Balaji, V.; Michl, J. *Polyhedron* **1991**, *10*, 1265.
- (11) Albinsson, B.; Teramae, H.; Plitt, H. S.; Goss, L. M.; Schmidbaur, H.; Michl, J. *J. Phys. Chem.* **1996**, *100*, 8681.
- (12) Teramae, H.; Michl, J. *Mol. Cryst. Liq. Cryst.* **1994**, *256*, 149.
- (13) Albinsson, B.; Teramae, H.; Downing, J. W.; Michl, J. *Chem. Eur. J.* **1996**, *2*, 529.
- (14) Tsuji, H.; Toshimitsu, A.; Tamao, K.; Michl, J. *J. Phys. Chem. A* **2001**, *105*, 10246.
- (15) Imhof, R.; Teramae, H.; Michl, J. *Chem. Phys. Lett.* **1997**, *270*, 500.
- (16) Crespo, R.; Teramae, H.; Antic, D.; Michl, J. *Chem. Phys.* **1999**, *244*, 203.
- (17) Crespo, R.; Merchán, M.; Michl, J. *J. Phys. Chem. A* **2000**, *104*, 8593.
- (18) Piqueras, M. C.; Crespo, R.; Michl, J. *Mol. Phys.* **2002**, *100*, 747.
- (19) Kendall, R. A.; Dunning, T. H., Jr.; Harrison, R. J. *J. Chem. Phys.* **1992**, *96*, 6796.
- (20) Frisch, M. J.; et al. *Gaussian 98, Revision A.7*; Gaussian Inc.: Pittsburgh, PA, 1998.
- (21) Widmark, P. O.; Persson, B. J.; Roos, B. O. *Theor. Chem. Acta* **1991**, *79*, 419.
- (22) Andersson, K.; Malmqvist, P. A.; Roos, B. O. *J. Chem. Phys.* **1992**, *96*, 1218.
- (23) Roos, B. O.; Taylor, P. R.; Siegbahn, P. E. M. *Chem. Phys.* **1980**, *48*, 157.
- (24) Finley, J.; Malmqvist, P. A.; Roos, B. O.; Serrano-Andrés, L. *Chem. Phys. Lett.* **1998**, *288*, 299.
- (25) Forsberg, N.; Malmqvist, P. A. *Chem. Phys. Lett.* **1997**, *274*, 196.
- (26) Andersson, K.; Blomberg, M. R. A.; Fulsher, M. P.; Karlstrom, G.; Lindh, R.; Malmqvist, P. A.; Neogrady, P.; Olsen, J.; Roos, B. O.; Sadlej, A. J.; Schutz, M.; Seijo, L.; Serrano-Andrés, L.; Siegbahn, P. E. M.; Widmark, P. O. *Molcas 5*, Department of Theoretical Chemistry, University of Lund, Lund, Sweden.
- (27) Haaland, A.; Rypdal, K.; Stüger, H.; Volden, H. V. *Acta Chem. Scand.* **1994**, *48*, 46.
- (28) Nelson, J. T.; Pietro, W. J. *J. Phys. Chem.* **1988**, *92*, 1365.
- (29) Ortiz, J. V.; Mintmire, J. W. *J. Am. Chem. Soc.* **1988**, *110*, 4522.
- (30) (a) Bock, H.; Ensslin, W.; Fehér, F.; Freund, R. *J. Am. Chem. Soc.* **1976**, *98*, 668. (b) Ortiz, J. V. *Polyhedron* **1991**, *10*, 1285. (c) Ortiz, J. V. *J. Chem. Phys.* **1991**, *94*, 6064. (d) Apeloig, Y.; Danovich, D. *Organometallics* **1996**, *15*, 350.
- (31) (a) Imhof, R.; Antic, D.; David, D. E.; Michl, J. *J. Phys. Chem. A* **1997**, *101*, 4579. (b) Fogarty, H. A.; David, D. E.; Ottosson, C.-H.; Michl, J.; Tsuji, H.; Tamao, K.; Ehara, M.; Nakatsuji, H. *J. Phys. Chem. A* **2002**, *106*, 2369.
- (32) (a) Plitt, H. S.; Michl, J. *Chem. Phys. Lett.* **1992**, *198*, 400. (b) Plitt, H. S.; Downing, J. W.; Raymond, M. K.; Balaji, V.; Michl, J. *J. Chem. Soc., Faraday Trans.* **1994**, *90*, 1653. (c) Schepers, T.; Michl, J. *J. Phys. Org. Chem.* **2002**, *15*, 490.